A Cleaning-Healing-Interfacial Polymerization Strategy for Upcycling Real End-of-Life PVDF Microfiltration Membranes

Ruobin Dai,[†] Hongyi Han,[†] Tianlin Wang,[†] Jiayi Li,[†] Zhichao Wu,[†] Chuyang Y. Tang,[‡] and Zhiwei Wang[*,†]

[†] State Key Laboratory of Pollution Control and Resource Reuse, Shanghai Institute of Pollution Control and Ecological Security, School of Environmental Science and Engineering, Tongji University, Shanghai 200092, China

[‡] Department of Civil Engineering, the University of Hong Kong, Pokfulam Road, Hong Kong S.A.R., China

[*] To whom all correspondence should be addressed.

Tel.: +86-21-65975669, Fax: +86-21-65980400, E-mail address: zwwang@tongji.edu.cn

Revised MS (R2) Submitted to: *ACS Sustainable Chemistry & Engineering* (July, 2021)

(Clean version)

ABSTRACT

Polyvinylidene fluoride (PVDF) microfiltration (MF) membranes, which are widely applied in the field of wastewater and water treatment, would inevitably reach their end-of-life (EOL) after numerous fouling-cleaning cycles. Lack of recycling strategy for the EOL PVDF MF membranes impedes the sustainability of membrane technology. In this study, we proposed a cleaning-healing-interfacial polymerization (IP) strategy to upcycle real EOL PVDF MF membranes from a membrane bioreactor for fabricating nanofiltration membranes. The cleaning step was responsible for removing most organic and inorganic foulants from the membrane, with a following healing step of membranes using polydopamine (PDA). After healing, a continuous and intact polyamide (PA) layer can be formed on the surface of the healed membrane via IP reaction between piperazine (PIP) and trimesoyl chloride. The PA nanofiltration (NF) membrane upcycled from the healed substrate (NF-Healed) membrane had a pure water permeance of 20.2 ± 1.1 L m^{-2} h^{-1} bar^{-1} and a Na_2SO_4 rejection of 92.4 ± 1.2%. The Na_2SO_4 permeability of NF-Healed membrane showed an approximately 2 orders of magnitude reduction in contrast to the NF membranes upcycled from the cleaned PVDF MF substrate, highlighting the critical role of PDA healing in conditioning the substrate. Detailed mechanistic investigation reveals that the PDA healing layer can avoid unfavorable growth of PA layer on hydrophobic PVDF substrate or cleaned substrates with low PIP uptake. The healing layer constructed a favorable hydrophilic platform for connection between PA oligomers and subsequent continuous growth of PA layer. This study provides an effective and robust protocol to upcycle EOL low-pressure membranes and reduce their environmental footprint.

KEYWORDS

End-of-life membrane, nanofiltration, polyamide layer, polydopamine healing, membrane recycling, surface hydrophobicity.

TOC Art

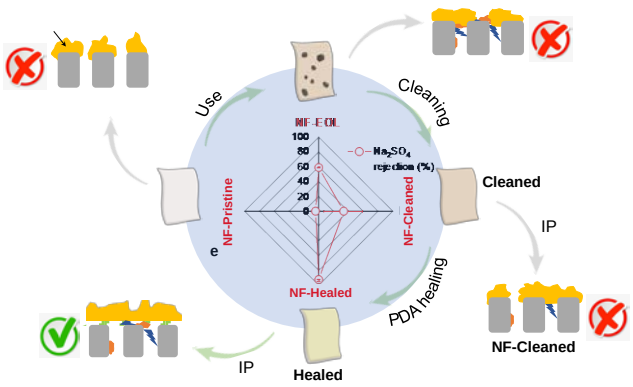

Synopsis: End-of-life PVDF microfiltration membranes were upcycled to new nanofiltration membranes via a novel three-step strategy, achieving sustainable use of membrane materials.

INTRODUCTION

Polyvinylidene fluoride (PVDF) microfiltration (MF) membranes have high mechanical strength, excellent chemical resistance and thermal stability,[1] leading to their wide applications in the field of water and wastewater treatment.[2-5] During their lifespan, PVDF MF membranes are subjected to numerous fouling-cleaning cycles. The damage of cleaning agents to membrane substrate and accumulation of irrecoverable foulants in PVDF matrix result in increased cleaning frequency and inability to meet flow throughput,[4,5] eventually leading to the end-of-life (EOL) of membranes (typically 5-10 years).[6,7] Currently, the disposal of EOL PVDF membranes is primarily via landfill.[8] With the global market for membrane components estimated to reach $20 billion by 2020,[9] nearly 30,000 tons of associated plastic waste need to be landfilled every year worldwide.[8] Due to the chemically stable nature of the PVDF materials[1], the landfill disposal of PVDF MF membranes has long-term negative environmental effects.

Environmental engineers and material scientists attempt to recycle EOL membranes.[7,10] Currently, most of the studies focus on the downcycling of EOL high-pressure membranes to obtain low-pressure membranes, *e.g.*, transforming EOL reverse osmosis (RO) membranes to nanofiltration (NF) or ultrafiltration (UF) membranes.[11,12] However, the research relating to the upcycling of EOL low-pressure membranes to prepare high-pressure membranes is quite scarce. In our recent study,[13] we found that a direct interfacial polymerization (IP) between amine and acyl chloride monomers could form polyamide (PA) rejection layers on biopolymer fouled MF substrates, which provides a strategy for upcycling fouled/EOL MF membranes. However, when this strategy was applied on the real EOL PVDF membranes during our pilot-scale experiments, it was noticed that the effectiveness cannot be ensured since the type and

distribution of foulants on the real EOL PVDF membranes varied significantly in different cases. Therefore, it prompts us to seek a more versatile strategy to upcycle the real EOL PVDF MF membranes.

We herein propose an upcycling strategy based on the features of the real EOL PVDF MF membranes. To avoid the interference of uneven distribution and varied type of foulants in real cases, the first step should be *cleaning* that can effectively remove a large part of the foulants (including both organic and inorganic foulants)[5]. Considering the exposed hydrophobic PVDF surface with inefficient uptake of amine monomer and possibly damaged membrane matrix during long-term use, the second step should be *healing*. The purpose of the healing step is to remediate the unfavorable sites that impede formation of continuous PA layer, e.g., due to weak uptake of reactive monomer. Polydopamine (PDA), which can be formed via self-polymerization of dopamine[14], is a kind of adhesive "bio-glue" that can strongly stick onto various natural surfaces[15]. Due to its catechol, quinone, and amine functional groups, PDA is highly hydrophilic[16] and therefore has the potential to heal the hydrophobic and possibly damaged surface of the cleaned PVDF membrane. The above cleaning and healing pretreatment steps ensure the quality of the final *interfacial polymerization* step to form a PA layer with enhanced and more consistent salt selectivity.

In this study, we demonstrated the cleaning-healing-IP strategy for upcycling real EOL PVDF MF membranes. These EOL PVDF membranes were thoroughly characterized after each step of cleaning, healing, and IP. By comparison among PA NF membranes upcycled from MF substrates after the different steps, we demonstrate the rationality and effectiveness of our strategy for upcycling real EOL PVDF MF membranes. We further reveal the critical roles of

the PDA healing on the growth of continuous and intact PA rejection layer on the real EOL membranes after chemical cleaning. This study provides a sustainable and promising pathway to upcycling real EOL MF membranes for preparing PA NF membranes.

MATERIALS AND METHODS

Real end-of-life PVDF MF membranes. Real EOL PVDF MF membranes (Supporting information, Figure S1) were obtained from a large-scale membrane bioreactor (MBR) in a municipal wastewater treatment plant, Shanghai, China. The membranes were used for the treatment of municipal wastewater for nearly 5 years and exposed to numerous fouling-cleaning cycles during the operation. Specifically, the membranes were exposed to *in-situ* NaOCl cleaning every month and *ex-situ* oxalic acid-NaOCl cleaning every six months. The EOL PVDF MF membranes (Brand name: TP7) was produced by Shanghai Zizheng Environmental Technology Co., Ltd. The pristine PVDF membrane (Figure S1) with a nominal pore size of 0.2 μm was also used for comparison.

Procedure of membrane upcycling. *Cleaning*: The real EOL PVDF MF membranes (denoted as EOL membranes) were first exposed to 0.5% (active chlorine) sodium hypochlorite solution for 2 h (Figure 1). After thoroughly washed by water, the membranes were immersed in 2 wt% oxalic acid solution for 2 h. The membranes after NaOCl and subsequent oxalic acid cleaning are denoted as cleaned membranes.

Healing: The cleaned membranes were then framed in a Teflon module (Figure S2) and exposed to 2 g/L dopamine hydrochloride dissolved in 10 mM Tris-HCl buffer solution (pH=8.5). The module containing the cleaned membranes was shaken (rotation speed of 80 rpm)

in the dark for 24 h to form polydopamine via self-polymerization. The membranes were subsequently removed from the module and washed by water to terminate the self-polymerization reaction, which were denoted as healed membranes.

Interfacial polymerization (IP): The healed membrane was further framed between two identical Teflon rings. The surface of the membrane was exposed to a 0.20 wt/v% piperazine (PIP)/water solution for 2 min. Excess PIP/water droplets were removed by a rubber roller. Immediately, a 0.16 wt/v% trimesoyl chloride (TMC)/n-hexane solution was poured onto the membrane surface for 30 s IP between PIP and TMC, to form a PA rejection layer. After pouring off the TMC/n-hexane solution, the as-synthesized thin-film composite (TFC) PA membrane was washed by water and cured in 60^{o}C oven for 5 min. The membranes, denoted as NF-Healed, were then stored in 4^{o}C deionized water for further use. Pristine, EOL, and cleaned PVDF membranes as controls were also subjected to the above IP, which were denoted as NF-Pristine, NF-EOL, and NF-Cleaned, respectively. The purpose of upcycling pristine, EOL, and cleaned PVDF membranes was to provide comparisons for us to better understand the role of each step and demonstrate the necessity and effectiveness of the cleaning-healing-IP strategy.

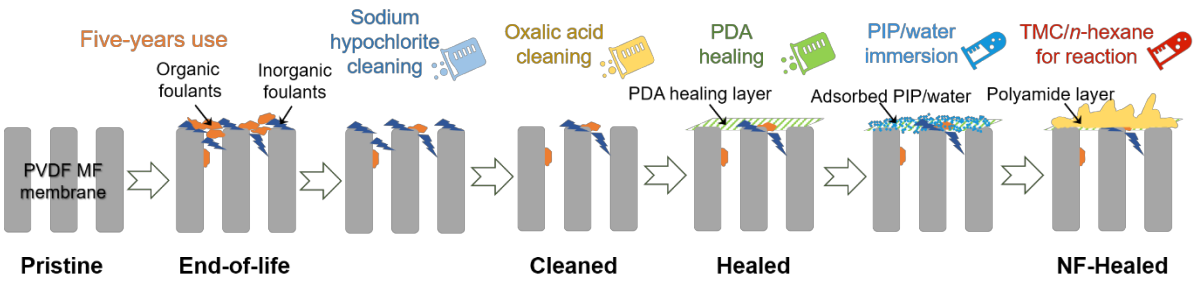

Figure 1. Schematic of the cleaning-healing-interfacial polymerization strategy for upcycling of real end-of-life PVDF MF membrane.

Synthesis of free-support polyamide films. In order to resolve the role of PDA healing on the growth of PA layer, we further synthesized PA films at a free interface between 0.20 wt/v% PIP/water and 0.16 wt/v% TMC/n-hexane and then transferred them onto various substrates (including pristine, EOL, cleaned, and healed MF membranes).[17,18] Briefly, a substrate was fixed on a Teflon platform in a glass container and was immersed in the PIP/water solution. The PIP/water level was 3 cm higher than the surface of the substrate to achieve formation of PA film at a free interface. The TMC/n-hexane solution was carefully poured onto the surface of PIP/water. The solution in the glass container was drained out via a pipe located at the bottom until the deposition of PA film on the substrate. The total reaction time for IP was 30 s. The resulting membrane was washed by water and cured in 60^{o}C oven for 5 min. Then the membrane was stored in deionized water at 4^{o}C.

Membrane characterization. The surface morphology of membranes was observed by a field-emission scanning electron microscope (FESEM, Nova Nano 450, FEI). Dried membrane coupons were coated with a thin layer of Pt before SEM characterization. The acceleration voltage for SEM observation was 5.0 kV. Membrane coupons were cut from EOL, cleaned, and healed membranes for confocal laser scanning microscope (CLSM, TCS SP8 STED 3X, Leica) observation. The polysaccharides and proteins on the membrane surface were labeled by Con A and SYPRO Orange, respectively.[19,20] The crystalline structure of foulants on PVDF membrane surface were characterized by X-ray diffraction (XRD). The PIP uptake of various PVDF membranes was expressed by the weight change after immersion in an aqueous solution of 0.05 wt/v % PIP for 2 min. Attenuated total reflectance-Fourier transform infrared

spectroscopy (ATR-FTIR), X-ray photoelectron spectroscopy (XPS), atomic force microscopy (AFM), zeta potential, and water contact angle measurements of the membranes were documented in our previous work.[21,22]

Membrane performance evaluation. The pure water permeance (PWP) of PVDF membranes were determined in a dead-end filtration cell (Millipore Amicon®, UFSC05001).[23] The water temperature was maintained at 25 °C. The PVDF membranes were pre-compacted at 50 kPa for 30 min before the formal measurement, and the PWP was determined at a constant pressure mode (30 kPa). Nanofiltration performance of upcycled TFC PA membranes was evaluated in a lab-scale cross-flow membrane filtration apparatus with an effective area of 9.1 cm^2.[22] A 10 L deionized water sample was recirculated for 4 h for membrane precompaction at 10 bar with a cross-flow velocity of 20.0 cm/s to stabilize the permeate flux. The feed solution temperature was kept constant at 25.0 ± 0.5°C. The water flux, dextrose rejection (40 mg/L), as well as rejection of single salts (10 mM Na_2SO_4, $MgCl_2$, $MgSO_4$, and NaCl) were measured at 8 bar. The dextrose concentration was determined by a total organic carbon analyzer (TOC-L, SHIMADZU), while the concentration of single salt was quantified by a conductivity meter (DDSJ-308F, INESA instrument).

RESULTS AND DISCUSSION

Cleaning of real end-of-life PVDF MF membranes. The top surface of real EOL PVDF MF membrane shows a brown color different from the pristine membrane (Figure 2a), indicative of the presence of a foulant layer on the membrane surface. The SEM images reveal that pores on

the membrane surface were totally covered by foulants for the EOL membrane (Figure 2a). The PWP of the EOL membrane (Figure 2b) was 280 ± 40 L m^{-2} h^{-1} bar^{-1}, which was significantly lower than that of the pristine membrane (1270 ± 50 L m^{-2} h^{-1} bar^{-1}).

After cleaning by sodium hypochlorite and oxalic acid, organic (e.g., polysaccharides and proteins) and crystalline inorganic foulants on the EOL membrane surface were mostly removed as indicated by CLSM and XRD characterizations (Figures S3 and S4), with many pores exposed on the membrane surface (Figure. 2a). ATR-FTIR spectrogram (Figure 2c) presents that the cleaning procedure eliminated the characteristic peak of 1653 cm^{-1}, which represents amino group in protein substances.[24] As shown in XPS spectra (Figure 2d), the decreased O1s and N1s signals as well as increased F1s signal after cleaning confirmed the removal of foulants from membrane surface.

Surprisingly, the PWP of the cleaned membrane recovered to 2070 ± 240 L m^{-2} h^{-1} bar^{-1} (Figure 2b), which was even higher than that of the pristine membrane. It implies a possible structural change for the cleaned membrane in contrast to the pristine membrane. The possible structural change was also reflected by the change in water contact angle of membrane surface (Figure 2e), which suggests that the cleaned membrane has a more hydrophobic surface than those of the pristine and EOL membranes. A more hydrophobic surface typically leads to a lower PWP for MF membranes.[25] However, the cleaned membrane had a PWP even higher than that of the pristine membrane, which can be explained by the significantly enlarged pore size (Figure S5). Moreover, we determined the PIP/water uptake of membranes (Figure 2e) as it directly affects the available PIP monomer on the membrane surface for IP. The cleaned membrane had a PIP uptake as low as that of the pristine membrane, which was widely noted

in literature[26,27]. It was reported that PA layer cannot directly formed on the hydrophobic surface of PVDF membranes unless applying surface modification or adding additives into the aqueous phase[26,27]. These results indicated that the matrix of cleaned membrane was damaged (or the pores were enlarged) and became more hydrophobic during fouling-cleaning cycles in the 5-year use, calling for a healing step to ensure quality of PA in IP process.

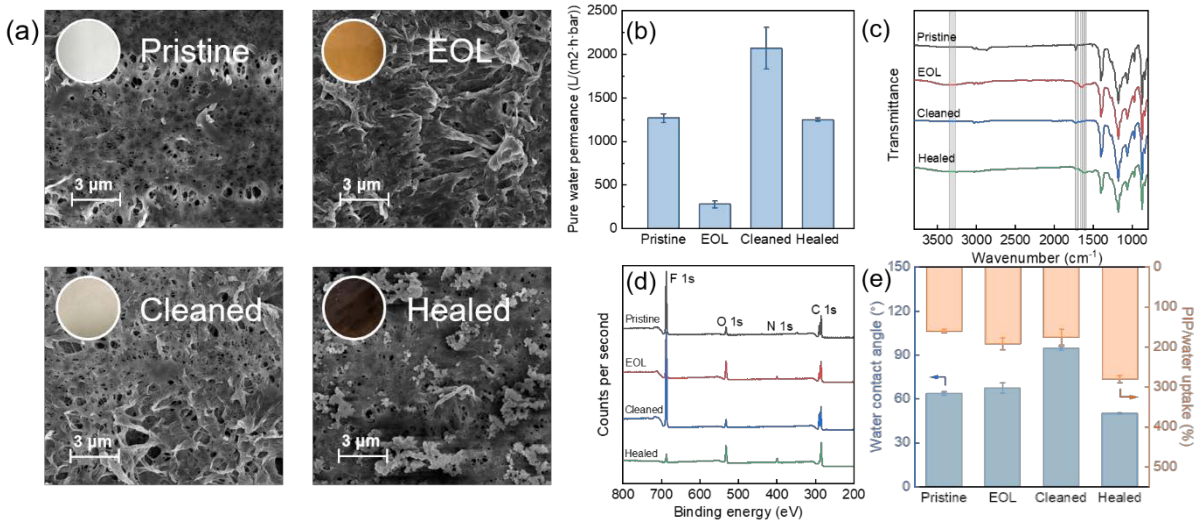

Figure 2. Characterization and performance of various PVDF MF membranes: (a) SEM images with corresponding digital photos at the upper left corners; (b) pure water permeance; (c) ATR-FTIR spectra; (d) XPS spectra; (e) water contact angle and PIP uptake. The PIP uptake represents the mass ratio of PIP absorbed by membrane.

Healing of real end-of-life PVDF MF membranes. Although chemical cleaning removed most foulants from the real EOL PVDF MF membranes, the possibly enlarged or even damaged membrane pores and more hydrophobic PVDF membrane surface for the cleaned membrane might impede effective sorption of PIP/water on membrane surface, which could lead to formation of defects in PA layer. Therefore, a healing step should be introduced between cleaning and further IP steps.

The surface of cleaned membrane was further healed by PDA via self-polymerization. Digital photo and SEM images (Figure 2a) display the formation of a PDA healing layer with a dark color. The PWP of the healed membrane was 1250 ± 20 L m^{-2} h^{-1} bar^{-1} (Figure 2b), which is comparable to that of the pristine membrane (Figure 2b) but lower than that of the cleaned membrane, corresponding to a decreased membrane pore size (Figure S5). A new peak at 1613 cm^{-1} for the healed membrane from ATR-FTIR spectra (Figure 2c) represents the overlap of C=C resonance vibrations in aromatic ring and N-H bending vibrations,[28] while the presence of broad peak centered around 3300 cm^{-1} corresponds to catechol OH groups,[29] which demonstrates formation of PDA on the healed membrane surface. The reduced F1s signal and increased O1s, N1s signals (Figure 2d) also confirm a coverage of PDA on the healed membrane surface.

The PDA healing significantly reduced surface water contact angle (Figure 2e) from 94.3 ± 1.5° (the cleaned membrane) to 49.7 ± 0.4° (the healed membrane), which is even lower than that of the pristine membrane (63.4 ± 1.1°). This effective surface hydrophilization can be attributed to the hydrophilic nature of PDA.[30] As expected, Figure 2e shows that the healed membrane had nearly 300% PIP/water uptake (*i.e.*, the healed membrane can absorb 300% PIP mass ratio of the membrane), which was higher than those of pristine, EOL, and cleaned membranes. Recent studies have shown that the substrate acts as a reservoir for aqueous monomers, with increased monomer uptake favored to form membranes of higher selectivity and/or water permeance.[31,32] The PDA modified substrates have a higher amine monomer uptake compared with conventional polysulfone (PSf) substrates[33].

Characterization of upcycled polyamide membranes. IP was performed on the healed membrane to form the PA rejection layer. The NF-Pristine, NF-EOL, and NF-Cleaned were also prepared as control samples. As shown in SEM images (Figure 3a), continuous PA layer cannot be formed on the pristine PVDF substrates, with a F1s peak detected by XPS (Figure S6), which implies exposure of substrate on the surface of NF-Pristine membrane. The discontinuity should be ascribed to the low PIP uptake induced by the hydrophobic nature of PVDF materials. In contrast, SEM images (Figure 3a) reveal that continuous PA layers can be formed on the EOL, cleaned and healed substrates with comparable surface roughness (Figure S7), while the NF-Healed membrane seems to have the most uniform surface appearance. ATR-FTIR results (Figure 3b) show characteristic peak of 1628 cm^{-1} (the amide I band),[34,35] confirming the formation of PA layers. A high-resolution deconvolution on O1s and N1s based on XPS analysis (Figure S6) for the NF-Healed membrane also demonstrates the formation of amide on the membrane surface (Figure 3c, d).

Figure 3e presents the O/N ratio and cross-linking degree of various membranes, both calculated from the XPS spectra (the calculation of cross-linking degree is detailed in Section S3). The O/N ratio of the NF-Healed membrane (1.23 ± 0.03) was significantly lower than those of NF-Pristine, NF-EOL, and NF-Cleaned membranes (2.31 ± 0.14, 1.53 ± 0.09, and 1.59 ± 0.21, respectively), revealing an increased cross-linking degree with the aid of PDA healing (69.5 ± 4.1% for the NF-Healed membrane). The cross-linking degree of the NF-Pristine membrane cannot be determined due to the large O/N value, which was ascribed to the discontinuity of its PA layer. The highest cross-linking degree for the NF-Healed membrane can be well explained by the enhanced PIP/water uptake by the healed PVDF MF substrate,

providing a higher concentration of PIP for IP process and thus forming a more cross-linked PA structure.[36] These results highlight the important role of PDA healing in formation of PA layer with high continuity and cross-linking degree.

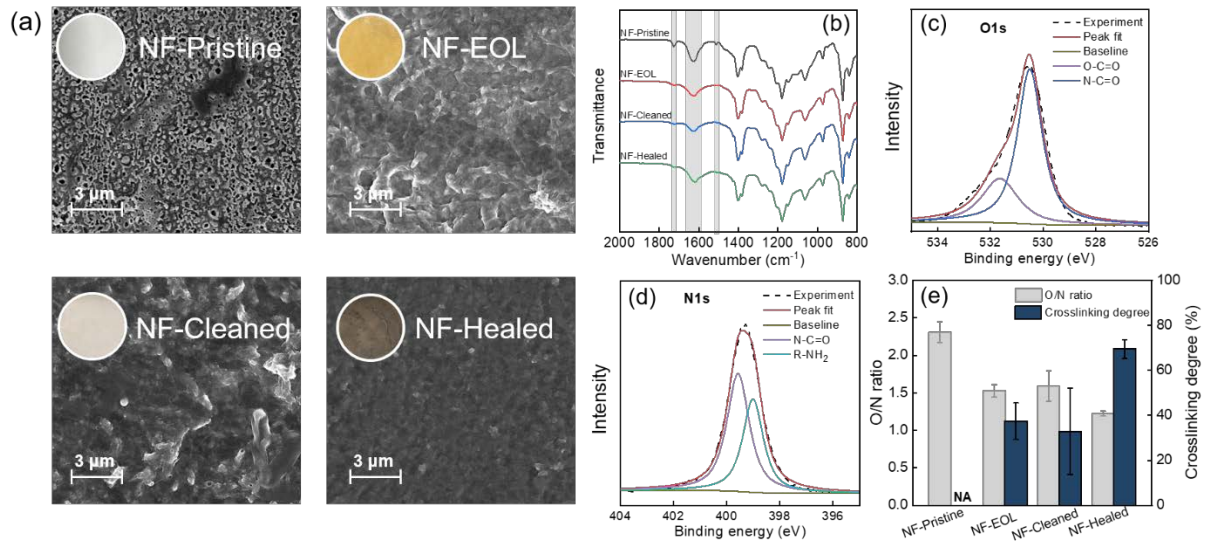

Figure 3. Characterization of TFC PA membranes upcycled from various PVDF MF substrates: (a) Surface morphology revealed by SEM observation; (b) ATR-FTIR spectra; (c) O 1s high-resolution spectra; (d) N 1s high-resolution spectra by XPS analysis for NF-Healed membrane and (e) O/N ratio and cross-linking degree of various membranes.

Nanofiltration performance of upcycled membranes. We further tested the nanofiltration performance of the upcycled membranes. Among various NF membranes, only NF-Healed membrane had the highest Na_2SO_4 rejection of 92.4 ± 1.2% (Figure 4a). The greatly improved Na_2SO_4 rejection for the NF-Healed membrane was primarily due to the formation of a more cross-linked PA rejection layer with better uniformity (Figure 3e). The NF-Pristine membrane has negligible Na_2SO_4 rejection, further demonstrating the unfavorable structure of PA layer on the pristine PVDF substrate. The NF-Cleaned membrane showed a Na_2SO_4 rejection and water

permeance with large error bar, implying the severe fluctuation of PA quality formed on the cleaned PVDF substrates. The fluctuation of PA quality was likely associated with both the unpredictable distribution of residual foulants after cleaning and possibly damaged PVDF membrane surface, impeding sufficient or uniform sorption of PIP/water on the surface of PVDF substrates and thus leading to possible formation of PA layer with defects. This result validates the necessity of PDA healing for obtaining a high-quality PA layer.

The PWP of the NF-Healed membrane is 20.2 ± 1.1 L m^{-2} h^{-1} bar^{-1}, which is comparable or higher than those of commercially available NF membranes and those prepared on conventional PES substrates (Figure S8). Although the PWP of NF-Pristine and NF-cleaned membranes were higher than that of the NF-Healed membrane, their compromised salt rejection hinders their applications. Moreover, as the permeate solute concentration is calculated by the ratio of solute flux over the water flux,[22,37] the salt concentration in the permeates of the NF-Pristine and NF-Cleaned membranes were actually "diluted" by the large water flux. The actual passage of Na_2SO_4 solutes across NF-Pristine and NF-Cleaned membranes are more severe than those expressed in the Na_2SO_4 rejection profile (Figure 4a). To avoid interference of the dilution effect, we calculated the Na_2SO_4 permeability and the results showed that the NF-Healed membrane had an approximately 1~3 orders of magnitude lower in Na_2SO_4 permeability compared to other membranes (Figure S9). This result reveals the critical importance of the PDA healing to obtain a continuous and intact PA layer for effective nanofiltration.

The nanofiltration performance of the NF-Healed membrane was further evaluated for rejection of various salts (Figure 4b). While the NF-Healed membrane performed nearly similar water permeance for all salts tested, the salt rejections for Na_2SO_4 and $MgSO_4$ were much

higher than those for $MgCl_2$ and NaCl. The rejection of charged salts by NF membranes were governed by the synergistic effect of size exclusion and Donnan exclusion. Dextrose, a neutral organic solute, was employed as the probe to evaluate the size exclusion effect by various membranes. Figure 4c shows that NF-Healed membrane had the highest dextrose rejection rate, which indicates an enhanced size exclusion effect thanks to the healing step. Moreover, zeta potential measurement (Figure 4d) suggests that NF-Healed membrane was strongly negatively charged at pH = 7 (with a zeta potential of ~ -50 mV). Both the increased size exclusion effect and strong Donnan exclusion resulted in high Na_2SO_4 rejection of the NF-Healed membrane.

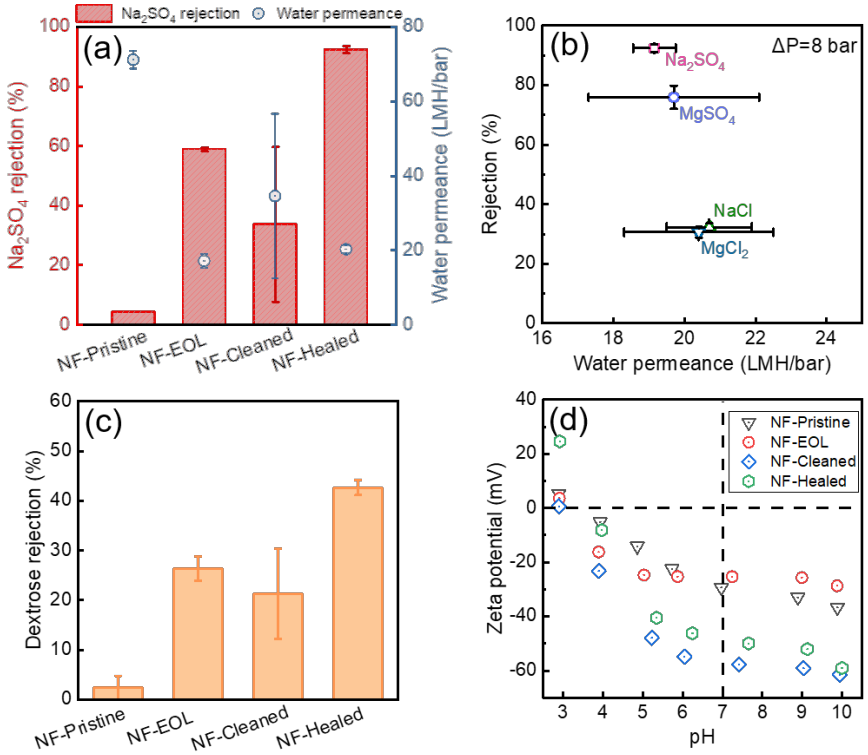

Figure 4. Performance of TFC PA membranes upcycled from various PVDF MF substrates: (a) Na_2SO_4 and water permeance; (b) single salts rejection by NF-Healed; (c) dextrose rejection; (d) zeta potentials.

The stability of the upcycled membranes is of great importance for practical application of

this upcycling strategy. The NF-Healed membrane maintained a constant flux without significant change in Na_2SO_4 rejection in long-term experiments performed over 144 h (Figure S10). Typically, NF membranes are fabricated based on polyether sulfone (PES) or PSf UF substrates. Assisted by the PDA healing, the NF membrane fabricated on PVDF MF substrate can extend its application to various extreme conditions (e.g., organic solvent-contained wastewater, high temperature wastewater), as the PVDF substrate has strong thermal stability, high mechanical strength, and excellent chemical resistance[27]. The role of PDA healing also implies that the cleaning-PDA healing-IP could potentially be a versatile method to upcycle various end-of-life membranes (various materials including PES, PSF and PVDF; membrane types including MF and UF; hydrophobic and hydrophilic).

Mechanistic insights. We further synthesized PA layers at a support-free interface between PIP/water and TMC/n-hexane solutions (rather than direct IP on substrates), and transferred the PA layers onto pristine, EOL, cleaned, and healed PVDF substrates. The NF membranes prepared at free-interface theoretically had identical PA rejection layers but different substrates. It allows us to understand the role of PDA healing, residual foulants, or the PVDF substrate itself in the separation performance of upcycled NF membranes, because it can avoid the effect of substrates on the growth of PA layer during IP reaction, i.e., the different PIP uptake conditions by various substrates.

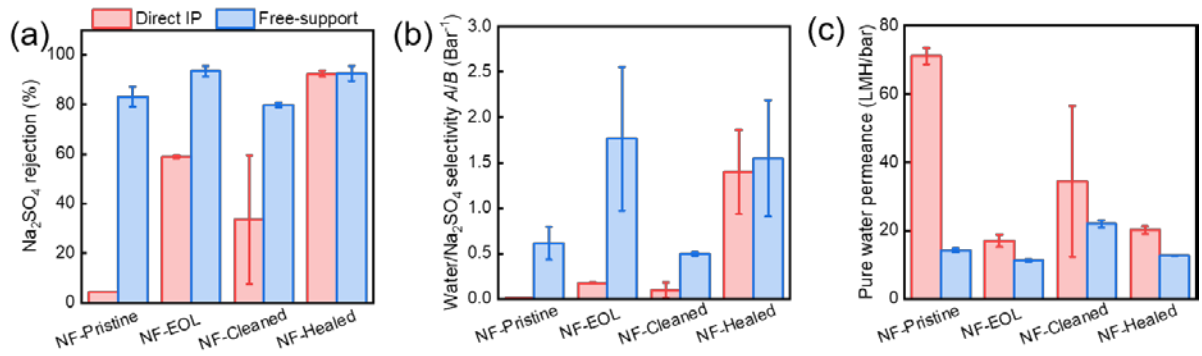

Figure 5. (a) Na_2SO_4 rejection, (b) water/Na_2SO_4 selectivity (A/B), and (c) pure water permeance of membranes prepared directly on various substrates, as well as those prepared at a free interface (and deposited on the substrates). Membrane performance was tested at an applied pressure of 8 bar at 25 °C.

Figures 5a,b present that only NF-healed membranes prepared by direct IP or free interface method have comparable Na_2SO_4 rejection and water/Na_2SO_4 selectivity ($A/B_{Na_2SO_4}$). The NF-Pristine, NF-EOL, and NF-Cleaned membranes prepared via direct IP all showed significantly lower Na_2SO_4 rejection and $A/B_{Na_2SO_4}$ than those prepared by free interface method, which meant that NF-Pristine, NF-EOL, and NF-Cleaned membranes prepared via direct IP had worser qualities of PA layers than those prepared by free interface method. It further confirmed that the unfavorable separation performance (Figure 4) of NF-Pristine, NF-EOL, and NF-Cleaned membranes was ascribed to the hydrophobic surfaces of the substrates incapable of providing enough amine monomer for formation of high-quality PA layer. For NF membranes prepared at free interface, their PWPs show a tendency of NF-Cleaned > NF-Pristine > NF-EOL ≈ NF-Healed (Figure 5c), which correspond well to the PWPs of MF substrates (Figure 2b). It implies that the resistance of substrates can directly determine the resistance of whole NF membranes when PA layers were identical.

Some previous studies showed that an interlayer (like the PDA healing layer in this study) between substrates and PA layer can induce a “gutter layer effect” (or called the direct effect in literature[33]) and the interlayer can reduce the whole membrane resistance to water[38,39]. However, we noticed that the NF-Healed membrane prepared at free interface had a lower PWP than that of the corresponding NF-Pristine membrane (Figure 5c), indicating that this study did not present a significant gutter layer effect even though a PDA healing on substrate was applied. Moreover, the NF-Healed membrane prepared by direct IP had a higher PWP than that of NF-Healed membrane prepared at free interface, which suggested that the PDA healing caused a positive effect in optimizing the IP process and structure of PA layer (or called the indirect effect in literature[33]), beyond facilitating the formation of continuous PA layer.

The comparison of membrane performance between direct IP and free interface demonstrated the critical importance of PDA healing on formation of high-quality, continuous, and intact PA layer. At initial stage of IP process, the instant reaction between PIP and TMC produces nuclei of PA materials, or PA oligomers, on substrates. The key of further formation of continuous PA layer with less defects is the connection of PA oligomers. However, on pristine PVDF substrate or cleaned substrate with uneven distribution of foulants, the PA oligomers cannot connect “hand in hand” (as drawn in Figure 6a) due to the relatively low PIP uptake (or low PIP density on the membrane surface). In contrast, the PDA healing layer conditions the surface to achieve enhanced PIP uptake, serving as a more favorable platform to “bridge” the PA oligomers into a continuous and high-quality PA layer (Figure 6b).

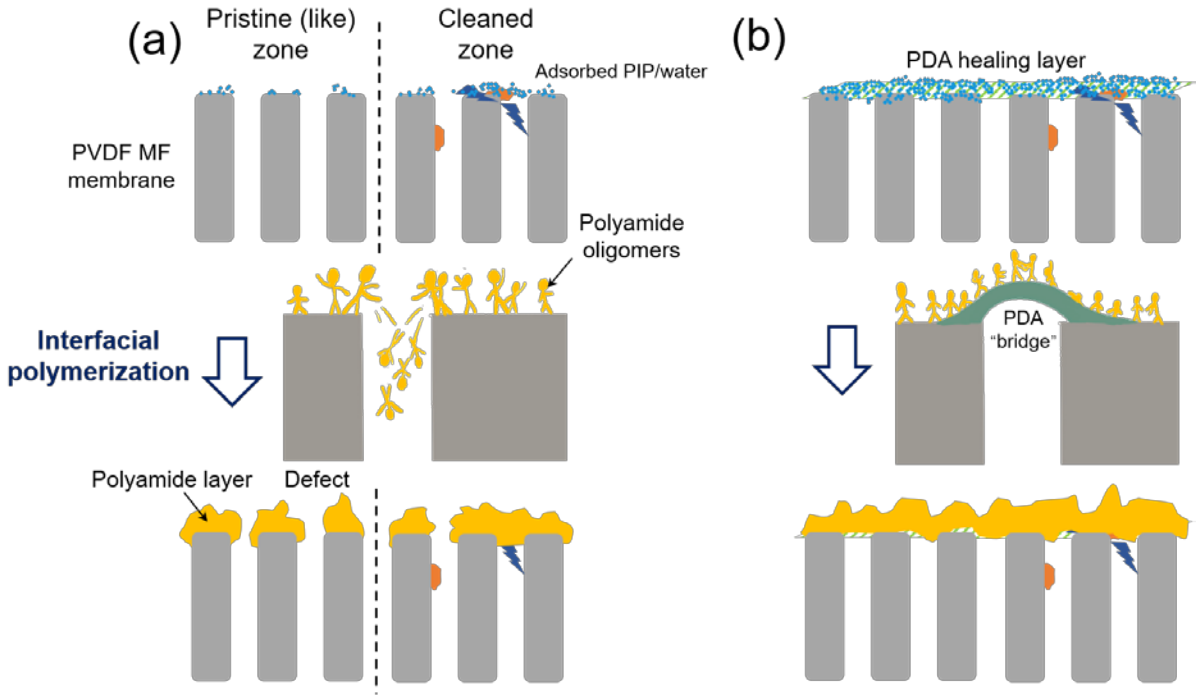

Figure 6. Schematics illustrating the role of PDA healing in formation of continuous PA layer on real end-of-life PVDF MF membranes.

Implications. For the first time, we proposed a cleaning-healing-IP strategy for upcycling real EOL PVDF microfiltration membranes. The cleaning, healing, and IP are responsible for foulant removal, reaction platform construction, and PA layer formation, respectively, allowing successful preparation of TFC PA membranes from EOL membranes for efficient nanofiltration. The strategy provides a robust route to form continuous and intact PA layer on the hydrophobic PVDF substrates with uneven distribution of foulants and possibly damaged surface. Moreover, the strategy can help address the issue of abandoned EOL low-pressure membranes, whose chemically stable nature makes their disposal quite harmful to the environment. By applying the strategy, the life span of the low-pressure membranes can be prolonged, which hence significantly reduces their environmental footprint. Although the membrane materials, foulants, and damaged conditions varied in different real cases, we believed that after proper

modifications (changing cleaning method, adjusting healing procedure, or optimizing the IP condition), the strategy can be used for upcycling EOL low-pressure membranes.

A major obstacle for applying this strategy to EOL low-pressure membranes in real applications is that traditional PA membrane production lines adopts continuous feeding of substrates. This in turn requires the dissemblance of membrane modules, which damages and wastes module housings, flow spacers, and interconnects, with major implications in overall economics and sustainability of the upcycling strategy. Therefore, novel and practical upcycling processes should be developed for *in-situ* cleaning, healing, and forming PA layer without destruction of membrane modules, for example, by using the concentration polarization enhanced modification technique.[40,41] Furthermore, the healing agent PDA in this study may be expensive and needs long reaction time (nearly 1 d), further development of a cheaper and more efficient healing agent is required in the future, for example, based on the metal-tannic acid chemistry[42].

CONCLUSIONS

A real EOL PVDF MF membrane was successfully upcycled to fabricate new NF PA membrane by a cleaning-PDA healing-IP strategy. The cleaning step was effective in removing most organic and inorganic foulants from the PVDF membrane. The PDA healing can avoid unfavorable growth of PA layer on hydrophobic PVDF substrate or cleaned substrates with low PIP uptake, constructing a favorable hydrophilic platform for connection between PA oligomers and subsequent continuous growth of PA layer. After the healing, a continuous and intact PA layer can be formed on the surface of healed PVDF membrane via IP reaction between PIP and

TMC. The NF-Healed membrane had a pure water permeance of 20.2 ± 1.1 L m^{-2} h^{-1} bar^{-1} and a Na_2SO_4 rejection of 92.4 ± 1.2%. The Na_2SO_4 permeability of NF-Healed membrane showed an approximately 2 orders of magnitude reduction in contrast to the NF membranes upcycled from the cleaned PVDF MF substrate, highlighting the critical role of PDA healing in conditioning the substrate. Our study provides an effective and robust protocol for sustainable use of EOL low-pressure membranes and reduce their environmental footprint.

ASSOCIATED CONTENT

Supporting information

The Supporting Information is available free of charge on the ACS Publications website at DOI: S1. Chemicals; Section S2. Basic calculations; Section S3. Calculation of cross-linking degree of membranes; Section S4. Photos of full-scale membrane bioreactor and flat-sheet membranes; Section S5. Teflon module for membrane healing; Section S6. CLSM images visualizing organic foulants on various MF membrane surfaces; Section S7. XRD characterizations of PVDF MF membranes; Section S8. Pore size distributions of various PVDF MF membranes; Section S9. XPS spectra of NF membranes upcycled from various PVDF MF membranes; Section S10. Surface roughness of NF membranes upcycled from various PVDF MF membranes; Section S11. Comparison of pure water permeances and Na_2SO_4 rejections of various membranes; Section S12. Solute permeability of NF membranes upcycled from various PVDF MF membranes; Section S13. Stability of the NF-Healed membrane.

AUTHOR INFORMATION

Corresponding Author

*Tel.: +86-21-65975669, Fax: +86-21-65980400, E-mail address: zwwang@tongji.edu.cn

Notes

The authors declare no completing financial interest.

ACKNOWLEDGMENTS

We thank the National Key R&D Program of China (2019YFC0408200) and the Science & Technology Commission of Shanghai Municipality (20DZ1207700). RBD would like to thank Shanghai Tongji Gao Tingyao Environmental Science & Technology Development Foundation for the financial support. CYT is partially supported by the Senior Research Fellow Scheme of the Research Grants Council of the Hong Kong Special Administrative Region, China (SRFS2021-7S04).

REFERENCES

(1) Liu, F.; Hashim, N. A.; Liu, Y.; Abed, M. R. M.; Li, K. Progress in the Production and Modification of PVDF Membranes. *Journal of Membrane Science* **2011**, *375* (1), 1–27. https://doi.org/10.1016/j.memsci.2011.03.014.

(2) Elimelech, M.; Phillip, W. A. The Future of Seawater Desalination: Energy, Technology, and the Environment. *Science* **2011**, *333* (6043), 712–717. https://doi.org/10.1126/science.1200488.

(3) Tang, C. Y.; Yang, Z.; Guo, H.; Wen, J. J.; Nghiem, L. D.; Cornelissen, E. Potable Water Reuse through Advanced Membrane Technology. *Environmental Science & Technology* **2018**, *52* (18), 10215–10223. https://doi.org/10.1021/acs.est.8b00562.

(4) Cote, P.; Alam, Z.; Penny, J. Hollow Fiber Membrane Life in Membrane Bioreactors (MBR). *Desalination* **2012**, *288*, 145–151. https://doi.org/10.1016/j.desal.2011.12.026.

(5) Wang, Z.; Ma, J.; Tang, C. Y.; Kimura, K.; Wang, Q.; Han, X. Membrane Cleaning in Membrane Bioreactors: A Review. *Journal of Membrane Science* **2014**, *468*, 276–307. https://doi.org/10.1016/j.memsci.2014.05.060.

(6) Coutinho de Paula, E.; Santos Amaral, M. C. Environmental and Economic Evaluation of End-of-Life Reverse Osmosis Membranes Recycling by Means of Chemical Conversion.

Journal of Cleaner Production **2018**, *194*, 85–93. https://doi.org/10.1016/j.jclepro.2018.05.099.

(7) Landaburu-Aguirre, J.; García-Pacheco, R.; Molina, S.; Rodríguez-Sáez, L.; Rabadán, J.; García-Calvo, E. Fouling Prevention, Preparing for Re-Use and Membrane Recycling. Towards Circular Economy in RO Desalination. *Desalination* **2016**, *393*, 16–30. https://doi.org/10.1016/j.desal.2016.04.002.

(8) Lejarazu-Larrañaga, A.; Molina, S.; Ortiz, J. M.; Navarro, R.; García-Calvo, E. Circular Economy in Membrane Technology: Using End-of-Life Reverse Osmosis Modules for Preparation of Recycled Anion Exchange Membranes and Validation in Electrodialysis. *Journal of Membrane Science* **2020**, *593*, 117423. https://doi.org/10.1016/j.memsci.2019.117423.

(9) Baker, R. W. *Membrane Technology and Applications*, 3rd ed.; John Wiley & Sons: Chichester, West Sussex ; Hoboken, 2012.

(10) García-Pacheco, R.; Lawler, W.; Landaburu-Aguirre, J.; García-Calvo, E.; Le-Clech, P. 4.14 End-of-Life Membranes: Challenges and Opportunities. In *Comprehensive Membrane Science and Engineering*; Elsevier, 2017; pp 293–310. https://doi.org/10.1016/B978-0-12-409547-2.12254-1.

(11) García-Pacheco, R.; Landaburu-Aguirre, J.; Molina, S.; Rodríguez-Sáez, L.; Teli, S. B.; García-Calvo, E. Transformation of End-of-Life RO Membranes into NF and UF Membranes: Evaluation of Membrane Performance. *Journal of Membrane Science* **2015**, *495*, 305–315. https://doi.org/10.1016/j.memsci.2015.08.025.

(12) Moradi, M. R.; Pihlajamäki, A.; Hesampour, M.; Ahlgren, J.; Mänttäri, M. End-of-Life RO Membranes Recycling: Reuse as NF Membranes by Polyelectrolyte Layer-by-Layer Deposition. *Journal of Membrane Science* **2019**, *584*, 300–308. https://doi.org/10.1016/j.memsci.2019.04.060.

(13) Dai, R.; Han, H.; Wang, T.; Li, J.; Tang, C. Y.; Wang, Z. Fouling Is the Beginning: Upcycling Biopolymer-Fouled Substrates for Fabricating High-Permeance Thin-Film Composite Polyamide Membranes. *Green Chem.* **2021**, *23* (2), 1013–1025. https://doi.org/10.1039/D0GC03340E.

(14) Lee, H.; Dellatore, S. M.; Miller, W. M.; Messersmith, P. B. Mussel-Inspired Surface Chemistry for Multifunctional Coatings. *Science* **2007**, *318* (5849), 426–430. https://doi.org/10.1126/science.1147241.

(15) Liu, Y.; Ai, K.; Lu, L. Polydopamine and Its Derivative Materials: Synthesis and Promising Applications in Energy, Environmental, and Biomedical Fields. *Chem. Rev.* **2014**, *114* (9), 5057–5115. https://doi.org/10.1021/cr400407a.

(16) Yang, H.-C.; Luo, J.; Lv, Y.; Shen, P.; Xu, Z.-K. Surface Engineering of Polymer Membranes via Mussel-Inspired Chemistry. *Journal of Membrane Science* **2015**, *483*, 42–59. https://doi.org/10.1016/j.memsci.2015.02.027.

(17) Jiang, Z.; Karan, S.; Livingston, A. G. Water Transport through Ultrathin Polyamide Nanofilms Used for Reverse Osmosis. *Adv. Mater.* **2018**, *30* (15), 1705973. https://doi.org/10.1002/adma.201705973.

(18) Zhu, J.; Hou, J.; Zhang, R.; Yuan, S.; Li, J.; Tian, M.; Wang, P.; Zhang, Y.; Volodin, A.; Van der Bruggen, B. Rapid Water Transport through Controllable, Ultrathin Polyamide Nanofilms for High-Performance Nanofiltration. *Journal of Materials Chemistry A* **2018**,

6 (32), 15701–15709. https://doi.org/10.1039/C8TA05687K.

(19) Chen, M.-Y.; Lee, D.-J.; Yang, Z.; Peng, X. F.; Lai, J. Y. Fluorecent Staining for Study of Extracellular Polymeric Substances in Membrane Biofouling Layers. *Environ. Sci. Technol.* **2006**, *40* (21), 6642–6646. https://doi.org/10.1021/es0612955.

(20) Yeon, K.-M.; Lee, C.-H.; Kim, J. Magnetic Enzyme Carrier for Effective Biofouling Control in the Membrane Bioreactor Based on Enzymatic Quorum Quenching. *Environ. Sci. Technol.* **2009**, *43* (19), 7403–7409. https://doi.org/10.1021/es901323k.

(21) Dai, R.; Zhang, X.; Liu, M.; Wu, Z.; Wang, Z. Porous Metal Organic Framework CuBDC Nanosheet Incorporated Thin-Film Nanocomposite Membrane for High-Performance Forward Osmosis. *Journal of Membrane Science* **2019**, *573*, 46–54. https://doi.org/10.1016/j.memsci.2018.11.075.

(22) Dai, R.; Guo, H.; Tang, C. Y.; Chen, M.; Li, J.; Wang, Z. Hydrophilic Selective Nanochannels Created by Metal Organic Frameworks in Nanofiltration Membranes Enhance Rejection of Hydrophobic Endocrine-Disrupting Compounds. *Environ. Sci. Technol.* **2019**, *53* (23), 13776–13783. https://doi.org/10.1021/acs.est.9b05343.

(23) Zhang, X.; Wang, Z.; Chen, M.; Liu, M.; Wu, Z. Polyvinylidene Fluoride Membrane Blended with Quaternary Ammonium Compound for Enhancing Anti-Biofouling Properties: Effects of Dosage. *Journal of Membrane Science* **2016**, *520*, 66–75. https://doi.org/10.1016/j.memsci.2016.07.048.

(24) Zhang, W.; Jiang, F. Membrane Fouling in Aerobic Granular Sludge (AGS)-Membrane Bioreactor (MBR): Effect of AGS Size. *Water Research* **2019**, *157*, 445–453. https://doi.org/10.1016/j.watres.2018.07.069.

(25) Zhang, X.; Wang, Z.; Chen, M.; Ma, J.; Chen, S.; Wu, Z. Membrane Biofouling Control Using Polyvinylidene Fluoride Membrane Blended with Quaternary Ammonium Compound Assembled on Carbon Material. *Journal of Membrane Science* **2017**, *539*, 229–237. https://doi.org/10.1016/j.memsci.2017.06.008.

(26) Zhang, Y.; Le, N. L.; Chung, T.-S.; Wang, Y. Thin-Film Composite Membranes with Modified Polyvinylidene Fluoride Substrate for Ethanol Dehydration via Pervaporation. *Chemical Engineering Science* **2014**, *118*, 173–183. https://doi.org/10.1016/j.ces.2014.07.040.

(27) Marquez, J. A. D.; Ang, M. B. M. Y.; Doma, B. T.; Huang, S.-H.; Tsai, H.-A.; Lee, K.-R.; Lai, J.-Y. Application of Cosolvent-Assisted Interfacial Polymerization Technique to Fabricate Thin-Film Composite Polyamide Pervaporation Membranes with PVDF Hollow Fiber as Support. *Journal of Membrane Science* **2018**, *564*, 722–731. https://doi.org/10.1016/j.memsci.2018.07.084.

(28) Jiang, J.-H.; Zhu, L.-P.; Li, X.-L.; Xu, Y.-Y.; Zhu, B.-K. Surface Modification of PE Porous Membranes Based on the Strong Adhesion of Polydopamine and Covalent Immobilization of Heparin. *Journal of Membrane Science* **2010**, *364* (1), 194–202. https://doi.org/10.1016/j.memsci.2010.08.017.

(29) Fei, B.; Qian, B.; Yang, Z.; Wang, R.; Liu, W. C.; Mak, C. L.; Xin, J. H. Coating Carbon Nanotubes by Spontaneous Oxidative Polymerization of Dopamine. *Carbon* **2008**, *46* (13), 1795–1797. https://doi.org/10.1016/j.carbon.2008.06.049.

(30) Guo, H.; Deng, Y.; Tao, Z.; Yao, Z.; Wang, J.; Lin, C.; Zhang, T.; Zhu, B.; Tang, C. Y. Does Hydrophilic Polydopamine Coating Enhance Membrane Rejection of Hydrophobic

Endocrine-Disrupting Compounds? *Environmental Science & Technology Letters* **2016**, *3* (9), 332–338. https://doi.org/10.1021/acs.estlett.6b00263.

(31) Yang, Z.; Zhou, Z.; Guo, H.; Yao, Z.; Ma, X.; Song, X.; Feng, S.-P.; Tang, C. Y. Tannic Acid/Fe $^{3+}$ Nanoscaffold for Interfacial Polymerization: Toward Enhanced Nanofiltration Performance. *Environmental Science & Technology* **2018**, *52* (16), 9341–9349. https://doi.org/10.1021/acs.est.8b02425.

(32) Peng, L. E.; Yao, Z.; Yang, Z.; Guo, H.; Tang, C. Y. Dissecting the Role of Substrate on the Morphology and Separation Properties of Thin Film Composite Polyamide Membranes: Seeing Is Believing. *Environ. Sci. Technol.* **2020**, *54* (11), 6978–6986. https://doi.org/10.1021/acs.est.0c01427.

(33) Yang, Z.; Wang, F.; Guo, H.; Peng, L. E.; Ma, X.; Song, X.; Wang, Z.; Tang, C. Y. Mechanistic Insights into the Role of Polydopamine Interlayer toward Improved Separation Performance of Polyamide Nanofiltration Membranes. *Environ. Sci. Technol.* **2020**, *54* (18), 11611–11621. https://doi.org/10.1021/acs.est.0c03589.

(34) Yang, Z.; Wu, Y.; Guo, H.; Ma, X.-H.; Lin, C.-E.; Zhou, Y.; Cao, B.; Zhu, B.-K.; Shih, K.; Tang, C. Y. A Novel Thin-Film Nano-Templated Composite Membrane with in Situ Silver Nanoparticles Loading: Separation Performance Enhancement and Implications. *Journal of Membrane Science* **2017**, *544*, 351–358. https://doi.org/10.1016/j.memsci.2017.09.046.

(35) Yang, Z.; Guo, H.; Yao, Z.; Mei, Y.; Tang, C. Y. Hydrophilic Silver Nanoparticles Induce Selective Nanochannels in Thin Film Nanocomposite Polyamide Membranes. *Environmental Science & Technology* **2019**, acs.est.9b00473. https://doi.org/10.1021/acs.est.9b00473.

(36) Li, Y.; Su, Y.; Li, J.; Zhao, X.; Zhang, R.; Fan, X.; Zhu, J.; Ma, Y.; Liu, Y.; Jiang, Z. Preparation of Thin Film Composite Nanofiltration Membrane with Improved Structural Stability through the Mediation of Polydopamine. *Journal of Membrane Science* **2015**, *476*, 10–19. https://doi.org/10.1016/j.memsci.2014.11.011.

(37) Yang, Z.; Guo, H.; Tang, C. Y. The Upper Bound of Thin-Film Composite (TFC) Polyamide Membranes for Desalination. *Journal of Membrane Science* **2019**, *590*, 117297. https://doi.org/10.1016/j.memsci.2019.117297.

(38) Yang, Z.; Sun, P.-F.; Li, X.; Gan, B.; Wang, L.; Song, X.; Park, H.-D.; Tang, C. Y. A Critical Review on Thin-Film Nanocomposite Membranes with Interlayered Structure: Mechanisms, Recent Developments, and Environmental Applications. *Environ. Sci. Technol.* **2020**. https://doi.org/10.1021/acs.est.0c05377.

(39) Dai, R.; Li, J.; Wang, Z. Constructing Interlayer to Tailor Structure and Performance of Thin-Film Composite Polyamide Membranes: A Review. *Advances in Colloid and Interface Science* **2020**, *282*, 102204. https://doi.org/10.1016/j.cis.2020.102204.

(40) Bernstein, R.; Belfer, S.; Freger, V. Improving Performance of Spiral Wound RO Elements by in Situ Concentration Polarization-Enhanced Radical Graft Polymerization. *Journal of Membrane Science* **2012**, *405–406*, 79–84. https://doi.org/10.1016/j.memsci.2012.02.046.

(41) Bernstein, R.; Belfer, S.; Freger, V. Bacterial Attachment to RO Membranes Surface-Modified by Concentration-Polarization-Enhanced Graft Polymerization. *Environ. Sci. Technol.* **2011**, *45* (14), 5973–5980. https://doi.org/10.1021/es1043694.

(42) Ejima, H.; Richardson, J. J.; Liang, K.; Best, J. P.; van Koeverden, M. P.; Such, G. K.; Cui, J.; Caruso, F. One-Step Assembly of Coordination Complexes for Versatile Film and Particle Engineering. *Science* **2013**, *341* (6142), 154–157. https://doi.org/10.1126/science.1237265.